*Sensors and Materials*, Vol. 37, No. 12 (2025) 5541–5559
MYU Tokyo


S & M 4262

# Developing a Taguchi and Backpropagation Network for Bitcoin Price Prediction

Chi-Han Chen,[1] Shui-Chuan Chen,[2*] and Wen-Zhe Hsu[2]

[1]Department of Industrial Education and Technology, National Changhua University of Education, Changhua 500207, Taiwan
[2]Department of Industrial Engineering and Management, National Chin-Yi University of Technology, Taichung 41170, Taiwan

(Received June 5, 2025; accepted December 4, 2025)

***Keywords:*** Taguchi method, backpropagation network (BPN), MATLAB, mean absolute percentage error (*MAPE*)

In this study, we investigate Bitcoin price volatility from December 15, 2014 to January 29, 2024 using an integrated, multisource feature set and an optimization–learning pipeline that couples Taguchi orthogonal arrays with a backpropagation network (BPN) implemented in MATLAB. Publicly available market variables were prioritized and nonquantifiable exogenous shocks were not modeled; Taguchi screening identified critical predictors and simultaneously tuned control factors (network specification, hidden-neuron count, and currency inclusion), after which the BPN was trained on aligned weekly ($n$ = 573) and monthly ($n$ = 108) datasets to ensure cross-market comparability. Model accuracy, assessed by mean absolute percentage error (*MAPE*), improved substantially after Taguchi-guided selection and configuration—weekly *MAPE* decreased from 3.23% to 0.36% and monthly *MAPE* from 6.32% to 0.07%—demonstrating the efficacy of the proposed optimization framework. Out-of-sample forecasts for February–April 2025 achieved predominantly sub-10% *MAPE*, while high-error instances were analyzed and attributed to contributing factors, yielding decision-relevant insights for practitioners and researchers. Collectively, the results show that systematic variable selection and orthogonal-array–based model design materially enhance neural forecasts of cryptocurrency prices and provide a reproducible pathway to accurate, time-efficient prediction.

## 1. Introduction

This study is aimed at investigating the key determinants influencing Bitcoin price volatility and at constructing an effective predictive model. Given the vast and complex nature of data within the cryptocurrency market, the processes of data acquisition, preprocessing, and variable selection are of critical importance. Accordingly, we will conduct a comprehensive review of pertinent literature related to the cryptocurrency domain, compare the effects of various explanatory variables on Bitcoin price behavior, and incorporate those indicators demonstrating

*Corresponding author: e-mail: scchen@ncut.edu.tw
https://doi.org/10.18494/SAM5774

ISSN 0914-4935 © MYU K.K.
https://myukk.org/

strong predictive capacity into the analytical framework. Moreover, for the development of the predictive model, we will utilize the backpropagation network (BPN) model in MATLAB to perform the analysis.[1] However, neural network models typically involve numerous hyperparameters that require fine-tuning, rendering the experimentation process both time-intensive and computationally demanding. To efficiently identify the optimal combination of parameters and input features, the Taguchi method implemented in Minitab will be employed.[2] This statistical approach enables the systematic evaluation of multiple parameters and their interactions with a reduced number of experiments. Furthermore, analysis of variance (ANOVA) will be conducted to identify the most statistically significant factors, thereby streamlining the model optimization process.[3] Referring to the experimental results derived from the Taguchi method, we will determine the parameter settings that yield optimal performance metrics for the predictive model. Given the complexity of the macroeconomic environment, we will exclude uncontrollable and exogenous factors such as changes in government regulations, natural disasters, and major financial disruptions that may induce volatility in the Bitcoin market. While minor fluctuations may be anticipated through historical data trends, unpredictable events such as natural catastrophes, wars, and economic conflicts can lead to substantial deviations in Bitcoin prices, thereby impairing forecasting accuracy.[4,5] Consequently, in this study, we will rely on established literature and focus on relatively stable and controllable variables. Specifically, five foreign exchange (forex) rates will be selected as the primary explanatory variables for analysis. The artificial neural network model will then be trained to predict Bitcoin price fluctuations. The model performance will be assessed using standard evaluation metrics, including mean squared error (*MSE*), root mean squared error (*RMSE*), and mean absolute percentage error (*MAPE*),[6,7] to identify influential variables and compute the model's predictive accuracy. Finally, a rolling analysis will be conducted to validate the robustness of the model, followed by a summary of findings and implications.

## 2. Related Studies

In this section, we introduce the relevant literature concerning the selection of financial variables across various asset classes, including cryptocurrencies, equities, bonds, mutual funds, futures, and other financial instruments. Particular emphasis is placed on prior empirical studies that have employed cryptocurrency as the target variable for forecasting, as they will serve as foundational references for the current research.[8–12] Kang *et al.*[8] proposed a hybrid model combining one-dimensional convolutional neural networks (1D-CNNs) with stacked gated recurrent units (GRUs) to forecast the price of cryptocurrencies. The CNN component extracts localized temporal patterns, while the GRU layers capture sequential dependencies across time. The model was applied to Bitcoin and Ethereum. It demonstrated superior performance in terms of *RMSE* compared with traditional LSTM and standalone CNN models. The results of Kang *et al.'s* provided empirical evidence supporting the efficacy of hybrid CNN-GRU architectures in capturing both spatial and temporal features in financial time series, contributing to the advancement of deep learning applications in financial forecasting. Qi *et al.*[9] developed a ConvLSTM-based predictive framework that fuses convolutional neural networks with LSTM cells, coupled with macroeconomic indicators, to inform cryptocurrency trading decisions of Bitcoin. This model demonstrates strong predictive capabilities for Bitcoin trading signals and highlights the significance of macroeconomic contexts in improving model interpretability. By integrating economic indicators into a spatiotemporal deep learning architecture, we successfully captured both spatial and temporal dependencies in Bitcoin price data. Karnati *et al.*[10] conducted a comparative analysis of classical and deep learning models—including ARIMA, Prophet, Support Vector Machines (SVMs), and LSTM—for Bitcoin price prediction. Among the tested algorithms, LSTM yielded the most accurate results across standard metrics (*RMSE*, *MAE*), owing to its ability to model nonlinear and sequential data patterns effectively. The research clarified the selection of appropriate time series forecasting models within the cryptocurrency domain, with implications for both retail and institutional investors. Ammer and Aldhyani[11] first used the deep-learning-based approach to forecast fluctuations in major cryptocurrencies including Ethereum, XRP, EOS, and AMP, with a focus on enhancing investor decision-making. Next, they applied LSTM to predict price fluctuations of multiple cryptocurrencies, achieving high prediction accuracy, especially with XRP, with correlation scores above 96%, outperforming traditional techniques in terms of precision and stability. Pellicani *et al.*[12] introduced the CARROT model, a multitask learning framework capable of detecting anomalies across groups of correlated cryptocurrencies in a unified fashion for simultaneous anomaly prediction across correlated cryptocurrencies. This model exhibits improved macro–F1-scores over individual anomaly predictors, especially in identifying regime shifts and atypical market conditions. It outperformed single-target models in macro–F1-score. Belcastro *et al.*[13] combined market data and social media sentiment in machine learning models to enhance the predictability of cryptocurrency prices. This proposed hybrid model significantly improved forecast accuracy and trading performance relative to single-source input models. By demonstrating the value of multisource data fusion, they expanded the methodological toolkit for data-driven trading strategies in the digital-asset space and provided improved decision support for traders, as evidenced by higher forecast accuracy and more stable risk-adjusted performance relative to single-source baselines.

In addition to the prediction of cryptocurrency, many scholars have studied the prediction function of the BPN and Taguchi method in different industries .[14-19] For example, Shie *et al.*[14] proposed a hybrid methodology in which the Taguchi method is integrated with an artificial neural network (ANN) for optimizing the solidification process parameters involved in artificial kidney manufacturing. The Taguchi method was used to design experiments and identify optimal factor combinations, while the ANN was trained on experimental data to build a predictive model for solidification performance. The integrated approach reduced the number of experimental trials while maintaining high predictive accuracy, thereby enhancing process efficiency and product quality. This research represents a significant advancement in biomedical manufacturing, demonstrating the effectiveness of combining the statistical design of experiments (DOE) with machine learning for complex bioengineering processes. Huang *et al.*[15] applied a four-stage hybrid methodology with a combination of the Taguchi method, response surface methodology (RSM), ANN, and genetic algorithm (GA) for robust process parameter optimization. Initial experiments were designed using the Taguchi method, followed by refinement with the RSM. The ANN modeled nonlinear interactions, and the GA was employed for global optimization. The hybrid framework significantly improved prediction accuracy and minimized the number of required experimental iterations. This research led to the establishment of a highly generalizable and reliable optimization framework especially suited for complex engineering systems involving nonlinear, multimodal response surfaces. Ouyang *et al.*[(16)] applied an intelligent parameter design framework, integrating the Taguchi method, to enhance the multi-objective performance characteristics (such as power density and fuel efficiency) of proton exchange membrane (PEM) fuel cell stacks. Through the Taguchi orthogonal array, key operating parameters were varied to evaluate their influence on multiple performance indices. A multi-objective optimization strategy was applied to interpret trade-offs. The analysis enabled the identification of parameter sets that simultaneously improved both energy efficiency and output stability. Li *et al.*[(17)] used an enhanced distributed parallel firefly algorithm (DPFA) optimized via the Taguchi method to improve diagnostic performance in transformer fault detection. The Taguchi method was employed to optimize the hyperparameters of the firefly algorithm. The improved algorithm was then used to train fault classifiers on diagnostic signal data. The Taguchi-optimized DPFA showed superior convergence speed and classification accuracy compared with conventional optimization approaches. Lin *et al.*[(18)] utilized the Taguchi method in conjunction with an ANN to optimize process parameters in resistance spot welding (RSW) to improve weld quality. The Taguchi-designed experiments were conducted to systematically assess the impact of input factors. A backpropagation ANN model was trained on the resulting data to forecast weld strength and nugget diameter. The combined method led to a statistically significant enhancement in both the mechanical and geometric qualities of welds. Zahlay and Rama Rao[(19)] proposed an adaptive automatic reclosure scheme for high-voltage transmission lines based on a hybrid Neuro-Prony model tuned using the Taguchi method. The Neuro-Prony model combines signal decomposition via Prony analysis and ANN-based classification to assess the post-fault system state. Taguchi DOE was utilized for the optimal tuning of control parameters. This proposed scheme successfully enhanced system resilience by reducing misoperation rates and improving recovery times under fault conditions.

## 3. Materials and Methods

### 3.1 Data

In this study, we examined a range of macro–financial indicators that may influence Bitcoin price fluctuations. Given that Bitcoin is legally traded in several major economies—such as the United States, India, and various European countries—and that the U.S. dollar (USD) is predominantly used as the base currency for valuation, the USD serves as the primary reference point for exchange rate conversion. Since Bitcoin operates as a decentralized digital asset and is actively traded 24 hours a day, 7 days a week—including weekends—there exists an inherent temporal mismatch between cryptocurrency trading and traditional fiat currency markets, which typically operate only during weekday business hours. To address this inconsistency and ensure uniformity in data granularity, daily cryptocurrency and exchange rate data were resampled and aggregated into weekly intervals. The data collection process involved retrieving historical Bitcoin price data and forex rates from the Investing.com platform and other statistical data repositories. The collected data were subsequently organized into weekly and monthly time frames for comparative and temporal analyses.

Table 1 presents a summary of the variables considered in the Taguchi and BPN model used in this study. The inclusion of forex rates from India, Brazil, Japan, Australia, and the European Union as explanatory variables in Bitcoin price modeling is underpinned by both macroeconomic relevance and geopolitical diversity. These regions represent a strategic mix of advanced economies and emerging markets, offering a broad spectrum of monetary policies, regulatory stances, and investor behaviors that may influence cryptocurrency valuation dynamics.

First, India is selected owing to its rapidly growing digital economy and high retail participation in cryptocurrency markets, despite an evolving and sometimes restrictive regulatory environment. The Indian rupee (INR) often reflects the sentiments of a vast demographic of users turning to Bitcoin as both a speculative asset and a hedge against local currency instability. Second, Brazil, as the largest economy in Latin America, offers a representative case of emerging markets where inflationary pressures and currency depreciation have led to increasing adoption of cryptocurrencies. The Brazilian real (BRL) captures regional macroeconomic volatility, providing insights into Bitcoin's role as a financial hedge in such economies. Next, Japan stands out as one of the most crypto-integrated nations globally. It was among the first countries to legally recognize Bitcoin and has developed a mature regulatory framework. The Japanese yen (JPY) is also one of the most traded fiat currencies globally, making it a critical factor in cross-market Bitcoin valuation. In addition, Australia contributes as a technologically advanced, financially transparent market with the early and continued adoption of blockchain technologies. The Australian dollar (AUD) serves as a proxy for Bitcoin's interaction with stable yet moderately sized developed economies, reflecting investor sentiment in the Asia-Pacific region. Finally, the European Union, represented by the Euro (EUR), plays a pivotal role in global finance. It is home to several of the world's leading economies and financial institutions. The Eurozone maintains a dynamic regulatory environment that increasingly engages with digital asset frameworks. As such, fluctuations in euro exchange rate are likely to capture broader macro–financial impacts on cryptocurrency markets.

Table 1
Selected variables.

| Nation | Currency |
|---|---|
| India | INR |
| Brazil | BRL |
| Japan | JPY |
| Australia | AUD |
| European Union | EUR |

### 3.2 Methods

The flowchart of our study procedure is illustrated in Fig. 1. We first develop a predictive model for Bitcoin price fluctuations on the basis of the selected financial indicators, utilizing a BPN to capture the inherent nonlinearity and volatility of cryptocurrency markets. The BPN model is configured through the careful calibration of key components, including the training algorithm, learning function, performance metric, number of neurons, and transfer functions. To evaluate the model's predictive capability, historical market data are employed as input to assess forecasting accuracy.

Furthermore, the Taguchi method is applied to efficiently reduce the dimensionality of the input variables and to identify optimal parameter settings, thereby minimizing experimental complexity while preserving model performance. Finally, the model's output is validated by

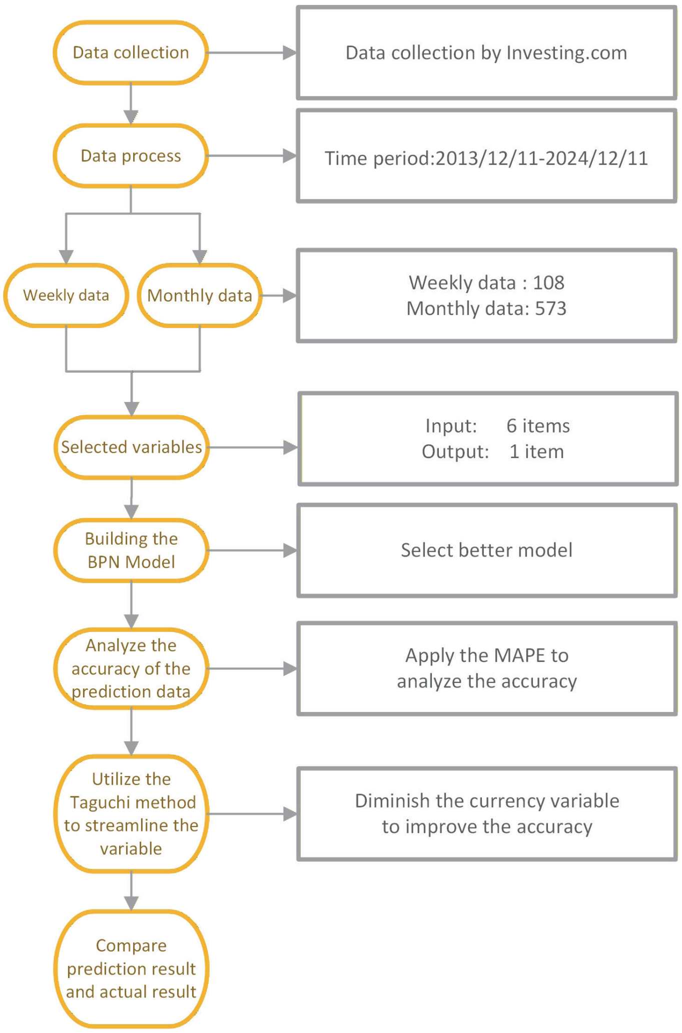


Fig. 1. (Color online) Research flowchart.

comparing predicted values derived from both weekly and monthly datasets against actual observed prices. Prediction accuracy is quantitatively assessed through performance metrics, enabling a comparative analysis between time-based data granularity and model precision.

### 3.3 BPN model

We utilize the MATLAB software because it is a high-level technical computing language widely recognized for its powerful capabilities in algorithm development, data analysis, numerical computation, and data visualization. It allows users to create customized graphical interfaces and supports the integration of external programming languages such as C and Java. One of MATLAB's key strengths lies in its extensive library of specialized toolboxes, each comprising a collection of functions tailored to specific domains. In this study, MATLAB R2019b, specifically, the Neural Network Toolbox (nntool), was employed to construct and simulate a predictive model using a BPN. The BPN is a supervised learning algorithm based on gradient descent optimization, wherein the network minimizes the error between predicted and actual outputs by adjusting weights in the direction of the negative gradient. The network architecture typically includes a hidden layer with nonlinear (e.g., tansig) activation functions and an output layer with linear (purelin) activation functions, allowing the network to approximate arbitrary nonlinear and even discontinuous functions.

In the modeling process, the input dataset (comprising selected influential variables) and corresponding target values (actual outcomes) were imported into nntool. The data were partitioned into training and testing samples, and formatted according to MATLAB's required input structure. These were assigned to the "Input Data" and "Target Data" fields, respectively. The network configuration was subsequently defined by specifying the number of hidden neurons, training functions (e.g., Levenberg–Marquardt or scaled conjugate gradient), learning functions, and performance functions (e.g., *MSE*). The proper selection of these parameters is essential, as they directly influence the model's convergence behavior and generalization performance. A poorly configured network may suffer from slow convergence, overfitting, or premature termination, whereas an optimally tuned network yields robust predictive accuracy.

The training process was initialized by setting key learning parameters, such as the learning rate and the maximum number of epochs. These configurations were visually represented through MATLAB's graphical outputs, including network diagrams and performance plots. The learning rate, in particular, plays a crucial role in convergence dynamics; an excessively high learning rate may lead to instability, while a very low learning rate can significantly prolong the training duration. Once the training process was completed, the model was evaluated using performance metrics, and the optimal network structure was retained for forecasting tasks. This integrated modeling framework demonstrates the effectiveness of MATLAB's neural network capabilities in constructing data-driven models for complex, nonlinear systems such as cryptocurrency price prediction.

### 3.3 Taguchi method

In this study, Minitab 17 was utilized to implement the Taguchi method for factor screening and model optimization in the development of a neural-network-based prediction model. As the Taguchi method is a structured experimental design technique under the broader framework of DOE, the process began by accessing the dedicated Taguchi design functions within Minitab's statistical analysis interface. Given the experimental structure consisting of three factors, each with three levels, an L9 orthogonal array was selected to efficiently investigate the influence of multiple variables while minimizing the number of required experimental runs. A stepwise elimination approach was employed to refine the experimental variables, which included key factors such as the number of hidden neurons, the type of neural network architecture, and the inclusion or exclusion of specific currency exchange rate variables as input features. These refined factors were designated as control factors within the orthogonal design. Through this systematic approach, the Taguchi method facilitated the identification of optimal parameter settings while simultaneously reducing model complexity. This not only enhanced the computational efficiency of the model training process but also contributed to improved prediction accuracy by isolating the most significant contributing factors.

### 3.4 Forecast evaluation criteria

To quantitatively assess the discrepancy between the predicted and actual values in this study, three widely recognized statistical performance metrics were employed: *MSE*, *RMSE*, and *MAPE*. These metrics serve as essential tools for evaluating the predictive accuracy and robustness of the developed neural network model. *MSE* measures the average squared difference between predicted and actual values, placing greater weight on larger errors and thus emphasizing model sensitivity to outliers. It is computed as

$$MSE = \frac{1}{n}\sum_{i=1}^{n}(y_i - \hat{y}_i)^2 , \tag{1}$$

where $y_i$ is the actual value, $\hat{y}_i$ is the predicted value, and $n$ is the number of observations.

*RMSE*, the square root of *MSE*, provides an interpretable error measure in the same units as the original data and is calculated as

$$RMSE = \sqrt{\frac{1}{n}\sum_{i=1}^{n}(y_i - \hat{y}_i)^2} . \tag{2}$$

*MAPE*, on the other hand, is a relative error metric that expresses forecast accuracy as a percentage. It is particularly advantageous because it is scale-independent and unaffected by the units of measurement, making it highly suitable for comparing different datasets or models. *MAPE* is defined as

$$MAPE = \frac{100\%}{n}\sum_{i=1}^{n}\left|\frac{y_i - \hat{y}_i}{y_i}\right|. \tag{3}$$

Given its interpretability and unit-free nature, *MAPE* was adopted as the primary indicator for prediction accuracy in this study. It enables the direct evaluation of estimation performance by indicating the average percentage deviation of predicted values from the actual observations. The classification of *MAPE* values into qualitative ranges further supports the objective assessment of model precision. To further support the interpretability of *MAPE* results, the following commonly used qualitative classification scheme is applied. This classification allows for a clearer understanding of the model's predictive quality and facilitates comparative assessment across alternative modeling configurations.

## 4. Results

Following the selection and preprocessing of relevant input variables, we proceeded to construct predictive models using a BPN framework, with both weekly and monthly datasets serving as inputs. The objective was to identify and quantify the key financial determinants influencing Bitcoin price fluctuations. The modeling process was conducted using MATLAB nntool, which was selected because of MATLAB's high computational efficiency, robust system modeling capabilities, and widespread applicability in engineering and data-driven research domains. The nntool offers several distinct advantages: (1) comprehensive algorithmic support for regression, classification, and dynamic system modeling using both shallow and deep learning architectures; (2) high-speed processing capabilities through integration with other toolboxes for scalable training and large-scale data handling; and (3) versatile training modes adaptable to different user applications, including time-series modeling with intermediate layer visualization and architecture customization.

### 4.1 Construct the BPN model

In this research, the Levenberg–Marquardt training algorithm (TRAINLM) was employed owing to its fast convergence properties and suitability for nonlinear function approximation. A network configuration comprising two hidden layers with ten neurons in each was adopted on the basis of the preliminary experimentation and parameter tuning. The training parameters were adjusted, as illustrated in Fig 2, to include a predefined stopping criterion aimed at optimizing the weight and bias updates to minimize prediction error. The input data samples were fed into the network through the MATLAB interface, and the predicted outputs were subsequently exported to Excel for post-analysis.

The accuracy of the model was evaluated using three key performance metrics: *MAPE*, *MSE*, and *RMSE*. The criteria for interpreting MAPE values, including the specific range indicating excellent prediction accuracy, are detailed in Table 2. The chosen training strategy and network configuration demonstrated strong predictive performance and provided a reliable foundation

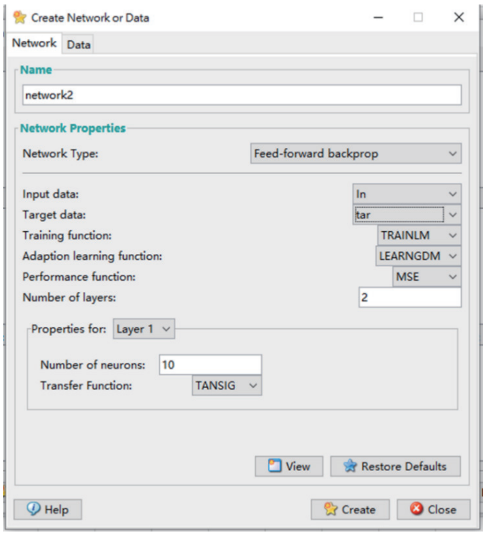


Fig. 2. (Color online) Interface for setting network mode.

Table 2
*MAPE* prediction accuracies.

| *MAPE* value (%) | Forecast accuracy |
|---|---|
| < 10% | Highly accurate forecasting |
| 10–20% | Good forecasting |
| 20–50% | Reasonable forecasting |
| > 50% | Inaccurate forecasting |

for identifying critical influencing factors in the Bitcoin market across different temporal granularities, as illustrated in Tables 3 and 4.

## 4.2 Training results

The evaluation results derived from both the weekly and monthly datasets indicate that the predictive model exhibits a high level of accuracy. Specifically, the *MAPE* values for the trained neural network were consistently below 10%, which, according to standard forecasting benchmarks, reflects high predictive precision. Furthermore, regression analysis revealed that the coefficient of determination ($R$) for the Training, Validation, Testing, and Overall data subsets closely approached a value of 1.0, signifying a strong linear correlation between the predicted outputs and the actual target values. This alignment of regression lines across all phases of the model training process confirms that the network has achieved effective convergence. The consistency of the regression plots underscores the model's robustness and generalization capability, thereby validating the effectiveness of the selected network architecture and training strategy in capturing the underlying patterns in the Bitcoin price data.

Table 3
Weekly forecast BPN model results.

| *MAPE* | *MSE* | *RMSE* |
|---|---|---|
| 3.23% | 4.6647 | 21.7594 |

Table 4
Monthly forecast BPN model results.

| *MAPE* | *MSE* | *RMSE* |
|---|---|---|
| 6.32% | 52.5534 | 7.2494 |

### 4.3 Improving weakly data forecasting results by the Taguchi method

To identify the optimal combination of input variables for Bitcoin price forecasting, we employed the Taguchi method. Each candidate variable was systematically excluded from the model to evaluate its contribution to prediction performance, thereby allowing for the identification of the most influential feature subset. The analysis was conducted using weekly data, providing a higher resolution for examining the relationship between foreign exchange rates and Bitcoin price trends. A series of simulation tests were executed using the proposed neural network architecture. Among the various configurations tested, the model trained with the Bayesian Regularization algorithm (TRAINBR) produced the lowest *MAPE* of 0.42%, indicating superior predictive precision. The BPN model factor results are summarized in Table 5.

Additional tests were conducted to investigate the effect of the number of hidden neurons, a critical factor in neural network design. The results revealed that a configuration with seven hidden neurons achieved the most favorable outcome, with a *MAPE* of 0.46%, suggesting that the model's accuracy is highly sensitive to architectural choices. The dataset was divided into training and testing subsets, and model evaluation was conducted using standard performance metrics including *MSE*, *RMSE*, and *MAPE*. The results for the number of neurons are summarized in Table 6.

A stepwise variable elimination procedure was implemented to further enhance model performance. The analysis showed that removing the Australian dollar (AUD) from the set of input variables yielded the most accurate model with a reduced *MAPE* of 0.40%. These finding highlights that not all financial indicators contribute equally to forecasting accuracy and that thoughtful variable selection, in combination with appropriate network tuning, is essential for achieving optimal predictive results. The results of deleting a variable are summarized in Table 7.

Following the application of stepwise elimination and adjustments to the number of hidden neurons, key factors influencing the prediction performance were systematically identified and organized for further analysis by the Taguchi method. Variables with higher forecasting accuracy—specifically, the number of hidden neurons, the type of neural network training algorithm, and the exclusion of certain currency exchange rates—were selected as control factors for constructing the experiment by the Taguchi DOE. We employed an L9 ($3^3$) orthogonal array to evaluate combinations of these factors. From the preliminary results, the optimal ranges

Table 5
Weekly data of BPN model factors.

| | *MAPE* | *MSE* | *RMSE* |
|---|---|---|---|
| **TRAINLM** | **3.23%** | **21.7594** | **4.6647** |
| TRAINCGB | 7.58% | 171.9401 | 13.1126 |
| TRAINSCG | 7.91% | 109.2451 | 10.4520 |
| **TRAINRP** | **7.48%** | **81.0478** | **9.0026** |
| TRAINOSS | 13.58% | 225.6220 | 15.0207 |
| TRAINCGP | 8.45% | 112.3210 | 10.5982 |
| TRAINCGF | 14.94% | 409.6046 | 20.2387 |
| **TRAINBR** | **0.42%** | **6.2267** | **2.4953** |

Table 6
Weekly data of number of neurons.

| | *MAPE* | *MSE* | *RMSE* |
|---|---|---|---|
| 2 neurons | 3.84% | 56.3321 | 7.5055 |
| **4 neurons** | **0.58%** | **1.0117** | **1.0058** |
| **5 neurons** | **1.09%** | **10.9885** | **3.3149** |
| 6 neurons | 1.63% | 33.9622 | 5.8277 |
| **7 neurons** | **0.46%** | **2.5795** | **1.6061** |
| 8 neurons | 1.88% | 64.8132 | 8.0320 |
| 9 neurons | 6.38% | 88.8729 | 9.4272 |
| 10 neurons | 3.23% | 21.7594 | 4.6647 |

Table 7
Weekly data of variable deletion.

| | *MAPE* | *MSE* | *RMSE* |
|---|---|---|---|
| ALL | 3.23% | 21.7594 | 4.6647 |
| **Deduct AUD** | **0.40%** | **0.8603** | **0.9275** |
| Deduct JPY | 3.57% | 26.4022 | 5.1383 |
| **Deduct INR** | **1.05%** | **2.9637** | **1.7216** |
| **Deduct EUR** | **2.93%** | **47.2488** | **6.8738** |
| Deduct BRL | 4.23% | 29.9098 | 5.4689 |

were determined to be 7, 8, and 10 hidden neurons, and three conditions for currency exclusion were as follows: excluding the Brazilian real, excluding the Indian rupee, and including all currencies. The factors and levels are summarized in Table 8.

Signal-to-noise (*S*/*N*) ratios were used to assess the robustness of each experimental run, with higher *S*/*N* ratios indicating higher model quality and lower loss. According to the results of *S*/*N* analysis, the best-performing configuration in terms of maximal *S*/*N* ratio was A3, B1, C3, corresponding to 7 hidden neurons, the TRAINLM training algorithm, and the exclusion of the EUR. However, further validation using main effects plots revealed that the optimal combination was A3, B1, C2, which corresponds to 7 hidden neurons, the TRAINLM algorithm, and the exclusion of the INR. The average *S*/*N* ratio levels for each factor also supported this result, confirming that this configuration yields the most stable and accurate forecasting outcome under the evaluated conditions. This analysis demonstrates the effectiveness of the Taguchi method in systematically optimizing the neural network structures and input feature selection to enhance predictive performance. The orthogonal table of weekly data is shown in Table 9.

Table 8
Weekly data of factors and levels.

| Level | A | B | C |
|---|---|---|---|
| | Factor | | |
| | Number of neurons | BPN model | Deleted variable |
| Level 1 | 4 | TRAINLM | AUD |
| Level 2 | 5 | TRAINRP | INR |
| Level 3 | 7 | TRAINCGB | EUR |

Table 9
Orthogonal table of weekly data.

| Number | A | B | C | Results | | | *S/N* |
|---|---|---|---|---|---|---|---|
| | | | | *MAPE* | *MSE* | *RMSE* | |
| 1 | 1 | 1 | 1 | 0.64% | 2.3467 | 1.5319 | 43.8764 |
| 2 | 1 | 2 | 2 | 5.57% | 54.1323 | 7.3574 | 25.0829 |
| 3 | 1 | 3 | 3 | 1.40% | 4.4027 | 2.0982 | 37.0774 |
| 4 | 2 | 1 | 2 | 0.37% | 0.7757 | 0.8807 | 48.6360 |
| 5 | 2 | 2 | 3 | 7.40% | 96.3241 | 9.8144 | 22.6154 |
| 6 | 2 | 3 | 1 | 1.64% | 5.7013 | 2.3877 | 35.7031 |
| **7** | **3** | **1** | **3** | **0.29%** | **1.5482** | **1.2442** | **50.7520** |
| 8 | 3 | 2 | 1 | 3.06% | 49.5744 | 7.0409 | 30.2856 |
| 9 | 3 | 3 | 2 | 1.15% | 7.0357 | 2.6525 | 38.7860 |

### 4.4 Improving monthly data forecasting results by the Taguchi method

Similar to the above, the monthly dataset constructed Taguchi-guided factor screening and aggregated at a monthly frequency, providing a higher resolution for examining the relationship between foreign exchange rates and Bitcoin price trends. A series of simulation tests were executed using the proposed neural network architecture. Among the various configurations tested, the model trained with TRAINCGF produced the lowest *MAPE* of 0.8%, indicating superior predictive precision. The monthly data of the BPN model factor are summarized in Table 10.

Additional tests were conducted to investigate the effect of the number of hidden neurons, a critical factor in neural network design. The results revealed that a configuration with ten hidden neurons achieved the most favorable outcome of a *MAPE* of 1.05%, suggesting that the model's accuracy is highly sensitive to architectural choices. The monthly data of the number of neurons are summarized in Table 11.

A stepwise variable elimination procedure was implemented to further enhance model performance. The analysis showed that removing the EUR from the set of input variables yielded the most accurate model, with a reduced *MAPE* of 0.65%. The monthly data of variable deletion are summarized in Table 12.

We employed an L9 ($3^3$) orthogonal array to evaluate the combinations of these factors. From the preliminary results, the optimal ranges were determined to be 10, 8, and 7 hidden neurons, and three conditions for currency exclusion were as follows: excluding the BRL, excluding the

Table 10
Monthly data of BPN model factors.

| | *MAPE* | *MSE* | *RMSE* |
|---|---|---|---|
| TRAINLM | 6.32% | 52.5534 | 7.2494 |
| TRAINCGB | 2.24% | 19.8156 | 4.4514 |
| TRAINSCG | 2.17% | 18.4536 | 4.2958 |
| **TRAINRP** | **1.59%** | **17.1623** | **4.1427** |
| TRAINCGP | 3.5% | 95.2647 | 9.7603 |
| **TRAINCGF** | **0.8%** | **2.7266** | **1.6512** |
| **TRAINBR** | **1.92%** | **140.6637** | **11.8601** |

Table 11
Monthly data of number of neurons.

| | *MAPE* | *MSE* | *RMSE* |
|---|---|---|---|
| 2 neurons | 6.32% | 52.5535 | 7.2494 |
| 4 neurons | 2.34% | 18.0043 | 4.2431 |
| 5 neurons | 2.46% | 27.9095 | 5.2829 |
| 6 neurons | 1.86% | 12.3036 | 3.5076 |
| **7 neurons** | **1.42%** | **5.8409** | **2.4168** |
| **8 neurons** | **1.16%** | **3.4167** | **1.8484** |
| 9 neurons | 1.43% | 10.7726 | 3.2821 |
| **10 neurons** | **1.05%** | **5.1609** | **2.2717** |

Table 12
Monthly data of variable deletion.

| | *MAPE* | *MSE* | *RMSE* |
|---|---|---|---|
| ALL | 0.89% | 2.7266 | 1.6512 |
| Deduct AUD | 2.67% | 33.7872 | 5.8126 |
| **Deduct JPY** | **0.87%** | **2.7930** | **1.6712** |
| **Deduct INR** | **1.04%** | **4.1872** | **2.0462** |
| **Deduct EUR** | **0.65%** | **4.0838** | **2.0208** |
| Deduct BRL | 1.06% | 8.2061 | 2.8646 |

AUD, and including all currencies. The monthly data factors and levels are summarized in Table 13.

According to the *S*/*N* analysis, the best-performing configuration in terms of maximal *S*/*N* ratio was A2, B3, C1, corresponding to 8 hidden neurons, the TRAINBR training algorithm, and the exclusion of the EUR. The orthogonal table of monthly data is shown in Table 14.

### 4.5 Experimental results and analysis

In the initial phase of this study, the dataset was divided into two segments, one for training and the other for out-of-sample simulation, to evaluate the model's predictive capability. Following model refinement using optimized input variables and neural network configurations, the results demonstrated notable improvements in forecasting accuracy. Specifically, the error values obtained using the updated results—summarized in Tables 15 and 16—were consistently

Table 13
Monthly data factors and levels.

| Level | A | B | C |
|---|---|---|---|
| | Factor | | |
| | Neuron numbers | BPN Model Factor | Deleted variable |
| Level 1 | 10 | TRAINCGF | EUR |
| Level 2 | 8 | TRAINRP | JPY |
| Level 3 | 7 | TRAINBR | INR |

Table 14
Orthogonal table of monthly data.

| Number | A | B | C | Results | | | *S/N* |
|---|---|---|---|---|---|---|---|
| | | | | *MAPE* | *MSE* | *RMSE* | |
| 1 | 1 | 1 | 1 | 1.53% | 17.7482 | 4.2128 | 36.3062 |
| 2 | 1 | 2 | 2 | 2.09% | 39.6225 | 6.2946 | 33.5971 |
| 3 | 1 | 3 | 3 | 1.43% | 82.5702 | 9.0868 | 36.8933 |
| 4 | 2 | 1 | 2 | 0.81% | 5.8838 | 2.4256 | 41.8303 |
| 5 | 2 | 2 | 3 | 3.38% | 21.6401 | 4.6518 | 29.4217 |
| **6** | **2** | **3** | **1** | **0.10%** | **0.1017** | **0.3190** | **60.0000** |
| 7 | 3 | 1 | 3 | 1.42% | 5.6697 | 2.3811 | 36.9542 |
| 8 | 3 | 2 | 1 | 5.92% | 51.3830 | 7.1681 | 24.5536 |
| 9 | 3 | 3 | 2 | 0.13% | 0.5565 | 0.7460 | 57.7211 |

Table 15
Weekly data before and after improvement.

| | *MAPE* | *MSE* | *RMSE* |
|---|---|---|---|
| Initial default settings | 3.23% | 4.6647 | 21.7594 |
| Adjustment of network training algorithm | 0.42% | 6.2267 | 2.4953 |
| Adjustment of the number of hidden neurons | 0.46% | 2.5795 | 1.6061 |
| Currency elimination approach | 0.40% | 0.8603 | 0.9275 |
| **Taguchi design – L9 orthogonal array** | **0.36%** | **4.0905** | **2.0224** |

Table 16
Monthly data before and after improvement.

| | *MAPE* | *MSE* | *RMSE* |
|---|---|---|---|
| Initial default settings | 6.32% | 52.5534 | 7.2494 |
| Adjustment of network training algorithm | 0.8% | 2.7266 | 1.6512 |
| Adjustment of the number of hidden neurons | 1.05% | 5.1609 | 2.2717 |
| Currency elimination approach | 0.65% | 4.0838 | 2.0208 |
| **Taguchi design – L9 orthogonal array** | **0.75%** | **3.0081** | **2.0897** |

lower across all evaluated performance metrics, including *MAPE*, *MSE*, and *RMSE*. This confirms the effectiveness of the model optimization process in enhancing predictive precision. Consequently, the final model, which incorporates the best-performing variable combination and neural network structure, will be applied to forecast Bitcoin prices on a weekly basis moving forward, providing a reliable foundation for ongoing prediction and analysis.

### 4.6 Evaluation of forecast accuracy by *MAPE* analysis between actual and predicted Bitcoin prices

In the preceding sections, we successfully identified the optimal neural network configuration through systematic adjustments of training algorithms, the number of hidden neurons, and the application of the Taguchi method.

These refinements led to the construction of a robust predictive model, which was subsequently applied to forecast future Bitcoin price trends. The weekly dataset comprised 573 data points collected from December 15, 2014, to January 29, 2024, while the monthly dataset included 133 data points over the same period. Moreover, utilizing the best-performing models as judged using the data in Table 17, predictive simulations were conducted through mid-April, encompassing Weeks 5 to 14 of 2025. The actual and predicted weekly closing prices for Bitcoin during this period were as shown in Table 17.

## 5. Discussion

Across the surveyed literature, methodological choices and data modalities are heterogeneous and evaluation criteria vary: Kang *et al.*[8] modeled timestamped closing prices with a 1D-CNN–GRU, reporting *RMSE* = 43.933; Qi *et al.*[9] integrated CMO, PPO, SAR, APO, and ROCP with ConvLSTM/SVM/Decision Tree, increasing an initial USD 1,000 to USD 36,798; Karnati *et al.*[10] used OHLC + market capitalization with LSTM, Facebook Prophet, ARIMA, and SVM and achieved an accuracy of 91%; Ammer and Aldhyani[11] forecast EOS via LSTM on OHLCV, yielding Pearson $r$ = 96.09%; Pellicani *et al.*[12] augmented OHLCV with the Fear-and-Greed index, feature expansion, and temporal clustering, whereby a multitarget LSTM improved the F1-score by 20% across 17 single-target models; Belcastro *et al.*[13] fused social-media signals, price volatility, causal structure, and sentiment using LSTM + dense layers and attained *MAPE* = 1.2%. In contrast, we combined multicurrency inputs (INR, BRL, JPY, AUD, and EUR) with a Taguchi-BPN optimization-learning framework and attained *MAPE* = 0.07%. These are summarized in Table 18.

Although the performance measures (*RMSE*, *MAPE*, F1, correlation coefficients, and capital growth) are not uniform across studies and hence preclude strict like-for-like comparisons, our approach exhibits state-of-the-art accuracy and superior inference latency. The exceptionally

Table 17
Weekly forecast prediction data and actual data obtained up to April 10, 2025.

| Week | Week 5 (2025) | Week 6 (2025) | Week 7 (2025) | Week 8 (2025) | Week 9 (2025) |
|---|---|---|---|---|---|
| Prediction data | 96767.528 | 101788.014 | 86482.5288 | 105150.48 | 109895.2078 |
| Actual data | 104000 | 106500 | 108200 | 110750 | 112300 |
| *MAPE* | 6.9543% | 4.4244% | 20.0716% | 5.0560% | 2.1414% |
| Week | Week 10 (2025) | Week 11 (2025) | Week 12 (2025) | Week 13 (2025) | Week 14 (2025) |
| Prediction data | 111871.5147 | 97304.5876 | 98363.8382 | 106686.8535 | 117214.8992 |
| Actual data | 113850 | 115400 | 116950 | 118500 | 120050 |
| *MAPE* | 1.7378% | 15.6806% | 15.8924% | 9.9689% | 2.3616% |

Table 18
Features of prediction models.

| Literature | Input variables | Method | Results |
|---|---|---|---|
| Kang *et al.*[8] | Timestamp, Date, Closing price | 1DCNN-GRU | *RMSE*<br>43.933 |
| Qi *et al.*[9] | CMO, PPO, SAR, APO, ROCP | ConvLSTM<br>SVM<br>Decision tree | Initial capital of USD 1000, grew to USD 36798 |
| Karnati *et al.*[10] | Date, Highest Price, Lowest Price, Opening Price, Closing Price, Market Cap | LSTM<br>Facebook Prophet<br>ARIMA<br>SVM | LSTM<br>91% |
| Ammer and Aldhyani[11] | Date, Highest Price, Lowest Price, Opening Price, Closing Price, Volume | LSTM | EOS currency<br>Pearson R rate 96.09% |
| Pellicani *et al.*[12] | OHLCV, Fear-and-Greed indicator, Feature Expansion | Temporal Clustering<br>Multitarget LSTM | All the 17 single-target LSTMs analyzed cryptocurrencies, with F1-score improvement of 20%. |
| Belcastro *et al.*[13] | Social media and price volatility, Causal relationship of market data, Sentiment analysis | LSTM<br>Dense Layers | *MAPE* 1.2% |
| This study | INR, BRL, JPY, AUD, EUR | Taguchi-BPN | *MAPE* 0.07% |

low *MAPE* reflects the precise tracking of price dynamics, while Taguchi-method-guided hyperparameter reduction and controlled model complexity shorten inference time, enhancing real-time decision utility and scalability across markets.

## 6. Conclusions

On the basis of the research findings, the following conclusions and contributions have been identified. First, we successfully applied neural network theories and methodologies to forecast Bitcoin prices using both weekly and monthly datasets. The experimental results demonstrated high predictive accuracy, underscoring the efficacy of neural networks as valuable tools in modeling and forecasting cryptocurrency price movements. Secondly, with variable selection and optimization, it was observed that not all variables significantly impact the predictive model. Therefore, the initial filtering of irrelevant variables is crucial to identify the optimal combination of predictors and enhance the model's performance. Next, the comparative analysis of different network training methods and various numbers of hidden neurons revealed that larger datasets necessitate an increased number of hidden neurons. Additionally, different training algorithms yielded varying results, indicating the importance of selecting the most suitable training method for specific predictive tasks. Finally, to improve the accuracy of the neural network model's output, we employed the Taguchi method for model adjustment. By considering network models, the number of hidden neurons, and the exclusion of certain currencies as control factors, the application of the Taguchi method led to improved predictive accuracy. We collected data on various national fiat currencies and Bitcoin from December 15, 2014, to January 29, 2024. Given that fiat currencies typically have trading days from Monday to

Friday, while Bitcoin operates 24/7, the data were converted into weekly and monthly datasets to ensure consistency and comparability for analysis.

Then, we focused on the weekly data, and after initial experiments and adjustments to variables and hidden neurons, *MAPE* decreased from 3.23% to 0.36%. For the monthly data, *MAPE* declined from 6.32% to 0.07% following similar adjustments. These improvements indicate that applying the Taguchi method to refine the neural network model significantly enhances predictive accuracy. We utilized the Taguchi method to enhance neural network models for forecasting Bitcoin prices. By analyzing 573 weekly data points and 108 monthly data points, our model provided forecasts for Bitcoin's trajectory from February to April 2025. The majority of the predicted *MAPE* values were below 10%, indicating high predictive accuracy. Instances where *MAPE* exceeded 10% were analyzed to identify contributing factors, offering valuable insights for investors. However, the Taguchi-method-guided neural-network framework delivers high accuracy and low inference latency for crypto-FX forecasting, yet several gaps remain: temporal aggregation may mask weekend dynamics; models are not regime-aware; drivers are correlational rather than causal; uncertainty and tail risk are unquantified; robustness across regimes is unclear; and explainability is limited. Future work should adopt multiresolution data fusion, regime detection with online adaptation, probabilistic forecasting (prediction intervals and calibrated quantiles), richer features (on-chain, options, order-book, and sentiment), and stronger baselines (Transformers/TFT/Informer) with principled tuning. Evaluation must extend beyond *MAPE* to directional accuracy, risk-adjusted PnL with costs, and latency under realistic deployment. Addressing these will translate high point accuracy into reliable, risk-aware, and scalable decision support.

## References


1 A. Stormy: MATLAB: A Practical Introduction to Programming and Problem Solving (Butterworth-Heineman, British, 2019) 4th–5th ed., pp. 3–35.
2 I. Alagić: Minitab Application as Statistical Tool for Lean Six Sigma (New Technologies, Development and Applications, Sarajevo, 2021) pp. 422–430.
3 R. Aniza, W. H. Chen, F.-C. Yang, A. Pugazhendh, and Y. Singh: Bioresour. Technol. **343** (2022) 126140. https://doi.org/10.1016/j.biortech.2021.126140
4 A. T. B. Duong, T. H. Hoang, T. T. B. Nguyen, M. Akbari, T. G. Hoang, and H. Q. Truong: J. Enterp. Inf. Manag. **36** (2023) 1372. https://doi.org/10.1108/JEIM-02-2023-0104
5 M. Dubyna, L. Verbivska, O. Kalchenko, V. Dmytrovska, D. Pilevych, and I. Lysohor: Int. J. Saf. Secur. Eng. **13** (2023) 821. https://doi.org/10.18280/ijsse.130506
6 A. Wan, Q. Chang, K. Al-Bukhaiti, and J. He: Energy **282** (2023) 128274. https://doi.org/10.1016/j.energy.2023.128274
7 Z. Zhao, S. Yun, L. Jia, J. Guo, Y. Meng, N. He, X. Li, J. Shi, and L. Yang: Eng. Appl. Artif. Intell. **121** (2023) 105982. https://doi.org/10.1016/j.engappai.2023.105982
8 C. Y. Kang, C. P. Lee, and K. M. Lim: Data. **7** (2022) 149. https://doi.org/10.3390/data7110149
9 Y. Qi, H. Jiang, S. Li, and J. Cao: Symmetry **14** (2022) 1896. https://doi.org/10.3390/sym14091896
10 V. Karnati, L. D. Kanna, T. N. Pandey, and C. K. Nayak: EAI Endorsed Trans. Internet Things **10** (2024). https://doi.org/10.4108/eetiot.5379
11 M. A. Ammer and T. H. H. Aldhyani: Electronics **11** (2022) 2349. https://doi.org/10.3390/electronics11152349
12 A. Pellicani, G. Pio, and M. Ceci: Expert Syst. Appl. **260** (2025) 125457. https://doi.org/10.1016/j.eswa.2024.125457
13 L. Belcastro, D. Carbone, C. Cosentino, F. Marozzo, and P. Trunfio: Algorithms **16** (2023) 542. https://doi.org/10.3390/a16120542

14 A.-J. Shie, K.-H. Lo, W. T. Lin, C. W. Juan, and Y. T. Jou: Biomed. Eng. Online **18** (2019) 78. https://doi.org/10.1186/s12938-019-0696-4
15 M.-L. Huang, Y.-H. Hung, and Z. S. Yang: Measurement **94** (2016) 284. https://doi.org/10.1016/j.measurement.2016.08.006
16 K. Ouyang, C. T. Li, and J. H. Chang: J. Taiwan Soc. Nav. Archit. Mar. Eng. **38** (2020) 135.
17 Z.-J. Li, W. G. Chen, J. Shan, Z.-Y. Yang, and L. Y. Cao: Energies **15** (2022) 3017. https://doi.org/10.3390/en15093017
18 H.-L. Lin, T. Chou, and C. P. Chou: Exp. Tech. **31** (2007) 30. https://doi.org/10.1111/j.1747-1567.2007.00186.x
19 F. D. Zahlay and K. S. Rama Rao: IEEE Trans. Power Del. **27** (2012) 575. https://doi.org/10.1109/TPWRD.2011.2182065

## About the Authors

**Shui-Chuan Chen** is currently a professor in the Department of Industrial Engineering and Management at National Chin-Yi University of Technology, where he also serves as the Dean of the College of Management. His research interests include process capability indices, neural network prediction models, Taguchi quality methods, the application of performance matrices, visual recognition, and the application of smart manufacturing. The courses he teaches include Enterprise Competition and Decision Analysis, Total Quality Management, International Quality Assurance, and Accounting. Recently, he published a paper in the journal Applied Sciences, on the topics of a fuzzy evaluation model of process improvement capability with costs consideration and statistical hypothesis testing for the asymmetric tolerance index. (scchen@ncut.edu.tw)

**Chi-Han Chen** is currently a doctoral student of the Graduate Institute of Industrial Education and Technology at National Changhua University of Education, Taiwan, Republic of China. He received his Bachelor's degree from National Taichung University of Science and Technology, Taiwan, and Master's degree from National Chin-Yi University of Technology, Taiwan. His current research interests include financial risk management, big data analysis, quality management, process yields index, Taguchi methods and application. (a0931132632@gmail.com)

**Wen-Zhe Hsu** received his B.S. degree from the Department of Industrial Engineering and Management, National Chin-Yi University of Technology, Taiwan, R.O.C., in 2021, and his Master's degree from the Department of Industrial Engineering and Management, National Chin-Yi University of Technology, Taiwan, R.O.C., in 2022. Since 2020, he has been an engineer at G-Tech Optoelectronics Corp. His research interests are in quality management, cost accounting, production management, and big data forecasting. (wenja1114@gmail.com)